



# An examination of parameterizations for the CCN number concentration based on in situ measurements of aerosol activation properties in the North China Plain

Z. Z. Deng<sup>1,2</sup>, C. S. Zhao<sup>2</sup>, N. Ma<sup>2</sup>, L. Ran<sup>1</sup>, G. Q. Zhou<sup>3</sup>, D. R. Lu<sup>1</sup>, and X. J. Zhou<sup>2,4</sup>

<sup>1</sup>Key Laboratory of Middle Atmosphere and Global Environment Observation, Institute of Atmospheric Physics, Chinese Academy of Sciences, Beijing, China

<sup>2</sup>Department of Atmospheric and Oceanic Sciences, School of Physics, Peking University, Beijing, China

<sup>3</sup>Shanghai Typhoon Institute, China Meteorological Administration, Shanghai, China

<sup>4</sup>Centre for Atmosphere Watch and Services, Chinese Academy of Meteorological Sciences, China Meteorological Administration, Beijing, China

Correspondence to: C. S. Zhao (zcs@pku.edu.cn)

Received: 10 November 2012 – Published in Atmos. Chem. Phys. Discuss.: 4 January 2013

Revised: 24 May 2013 – Accepted: 27 May 2013 – Published: 1 July 2013

**Abstract.** Precise quantification of the cloud condensation nuclei (CCN) number concentration is crucial for understanding aerosol indirect effects and characterizing these effects in models. An evaluation of various methods for CCN parameterization was carried out in this paper based on in situ measurements of aerosol activation properties within HaChi (Haze in China) project. Comparisons were made by closure studies between methods using CCN spectra, bulk activation ratios, cut-off diameters and size-resolved activation ratios. The estimation of CCN number concentrations by the method using aerosol size-resolved activation ratios, either averaged over a day or with diurnal variation, was found to be most satisfying and straightforward. This could be well expected since size-resolved activation ratios include information regarding the effects of size-resolved chemical compositions and mixing states on aerosol activation properties. The method using the averages of critical diameters, which were inferred from measured CCN number concentrations and particle number size distributions, also provided a good prediction of the CCN number concentration. Based on comparisons of all these methods in this paper, it was recommended that the CCN number concentration be predicted using particle number size distributions with inferred critical diameters or size-resolved activation ratios.

## 1 Introduction

Clouds have an impact on the global water cycle by cloud formation and precipitation as well as on the energy balance of the earth–atmosphere system by absorption, scattering and emission of radiation. Cloud condensation nuclei (CCN), i.e. the particles that can be activated at a certain water vapor supersaturation, could influence cloud microphysical properties. An increase in CCN number concentration may increase the cloud droplet number concentration (Twomey and Warner, 1967; Ramanathan et al., 2001), and decrease the size of cloud droplets (Twomey, 1974), consequently further change cloud lifetime and precipitation (Albrecht, 1989; Zhao et al., 2006b). Thus, the CCN number concentration is a key factor to characterise aerosol indirect effects, i.e. the impacts of aerosols as CCN on climate.

CCN number concentrations and CCN spectra have been characterised by field measurements since the 1950s (Twomey, 1959a, and reference therein). Measurements in various locations and seasons showed that CCN number concentrations were generally higher in the continental air (Delene and Deshler, 2001; Detwiler et al., 2010; Rose et al., 2010; Deng et al., 2011; Gunthe et al., 2011) than in the maritime air (Squires and Twomey, 1966; Bigg and Leek, 2001), and higher under polluted conditions than under clean conditions (Hobbs et al., 1980; Snider and Brenguier, 2000; Hudson et al., 2000; Hudson and Yum, 2002). With such high

spatial and temporal variability in CCN properties, robust parameterization of the CCN number concentration is of great importance to model applications.

Several parameterization schemes of the CCN number concentration have been developed. The parameterization of CCN spectra with constants (Twomey, 1959b; Ji and Shaw, 1998; Mircea et al., 2005), though simple to carry out, does not take into account any variation in the CCN loading. The bulk activation ratio (the ratio between CCN and aerosol number concentrations) was also a useful parameter in the CCN prediction (Pruppacher and Klett, 1997). Measurements and sensitivity studies indicated that the particle size plays a more important role in the aerosol activation process at high supersaturations than the chemical composition does (Junge and McLaren, 1971; Fitzgerald, 1973; Dusek et al., 2006), which could however be quite important at low supersaturations (Kuwata et al., 2008; Twohy and Anderson, 2008). Closure studies of the CCN number concentration based on the particle number size distribution (PNSD) were conducted to investigate the influence of bulk (Bougiatioti et al., 2009) and size-resolved aerosol chemical compositions (Medina et al., 2007; Stroud et al., 2007). The effects of aerosol mixing states on the CCN prediction were also notable in locations with strong anthropogenic aerosol emissions (Ervens et al., 2010; Kammermann et al., 2010; Rose et al., 2010; Wang et al., 2010; Wex et al., 2010; Deng et al., 2011; Kerminen et al., 2012). The examination of these methods for the CCN calculation can be used to considerably improve the parameterization of the CCN number concentration.

Measurements of aerosol optical properties (Ma et al., 2011, 2012), aerosol hygroscopicity (Liu et al., 2011) and aerosol activation (Deng et al., 2011) during the Haze in China (HaChi) campaign have shown that the North China Plain (NCP) is one of the most heavily polluted regions in the world, wherein a variety of strong aerosol emission sources are located. Studies show that high concentration of aerosol particles in these region may have impacts on cloud microphysical properties and surface precipitation (Zhao et al., 2006a, b; Deng et al., 2009). Under such polluted circumstances, parameterizations of CCN might be somewhat different from usual methods. Precise quantification of CCN number concentration is required in detailed cloud models, where the activation fraction of aerosols depend nonlinearly on the aerosol abundance. Thus, it is necessary to examine the validity of the CCN parameterization schemes. Intensive measurements of aerosol activation properties in this study were employed to evaluate different methods for CCN parameterizations, including the use of CCN spectra, bulk CCN activation ratios, cut-off diameters and size-resolved activation ratios (activation curves).

## 2 Measurements and data

Measurements of PNSD and aerosol activation properties were conducted at Wuqing Meteorological Station from 5 November to 30 December 2011. More information on the site and the polluted surrounding areas were described in Xu et al. (2011) and Ran et al. (2011). Number size distributions and activation properties of aerosols dried to less than 30 % relative humidity were measured by an aerodynamic particle sizer (APS Model 3320, TSI, USA), a scanning mobility particle sizer (SMPS, Model 3936, TSI, USA) and a continuous-flow CCN counter (CCNC, Model CCN-200, DMT, USA) (Roberts and Nenes, 2005; Lance et al., 2006).

The SMPS consisted mainly of a differential mobility analyser (DMA, Model 3081, TSI, USA) and a condensation particle counter (CPC, Model 3772, TSI, USA). The DMA sheath and sample flows were 6 Lpm and 0.8 Lpm, respectively. The sample flow exiting the DMA was split into two parts, with 0.3 Lpm for CPC and 0.5 Lpm for one column of the CCNC. The DMA, controlled by the TSI-AIM software, scanned a cycle every five minutes and selected particles in a certain size increment between 10–430 nm. The PNSD and size-resolved activation properties were obtained by using this scanning system (Moore et al., 2010). The PNSD was inverted from the raw counts recorded by AIM using an algorithm (Hagen and Alofs, 1983; Wiedensohler et al., 2012) with the ideal Dirac, triangular transfer function (Knutson and Whitby, 1975) and the particle equilibrium charge probability distribution (Wiedensohler, 1988). The PNSD in the range of 10 nm–10  $\mu$ m were obtained in combination with APS measurements.

The CCNC column downstream of the DMA was operated at five supersaturations, with 20 min for 0.07 % and 10 min each for 0.10, 0.20, 0.40 and 0.80 %. The chamber of the CCNC was considered as temperature stabilised during the last 5 min of the duration for each supersaturation. The time series of size-selected CCN number concentrations ( $N_{CCN,s}(D_p,S)$ ) during these 5 min were matched with the size-selected CN (Condensation Nuclei) number concentrations ( $N_{CN,s}(D_p)$ ) measured with the CPC. The size-resolved aerosol activation ratios ( $A(D_p,S) = N_{CCN,s}(D_p,S)/N_{CN,s}(D_p)$ ) were inverted from size-selected CCN number concentrations and PNSD using a modified algorithm based on Hagen and Alofs (1983). The size-resolved activation ratios for five supersaturations were available every one hour. The sheath and sample flow rates of CCNC were calibrated before the campaign. The supersaturations of CCNC were calibrated with ammonium sulfate (Rose et al., 2008) before and after the campaign. The results showed that the effective supersaturations were 0.061, 0.083, 0.200, 0.414 and 0.812 %.

The other column of the CCNC was used to measure total CCN number concentrations at supersaturations of 0.07, 0.10, 0.20, 0.40 and 0.80 %, of which direct measurements could lead to considerable underestimations under polluted

conditions (Deng et al., 2011) due to water depletion inside the column (Latham and Nenes, 2011). Number size distributions of CCN were constructed by multiplying the PNSD and corresponding size-resolved activation ratios. The bulk CCN number concentrations were the integration of the CCN number size distribution, and referred to as measured CCN number concentration in the following content.

### 3 Calculation of CCN number concentrations

The methods for CCN parameterizations, including the use of CCN spectra, bulk CCN activation ratios, cut-off diameters and size-resolved activation ratios, are described and compared below to characterise the variations of CCN number concentrations.

#### 3.1 Parameterization of CCN spectra using aerosol number concentration

The method that uses only CCN spectra for the CCN parameterization provides a simple way to predict CCN number concentrations, with very few constants required for modelling. CCN supersaturation spectra have often been measured and fitted with different formulas. A commonly used formula,

$$N_{\text{CCN}}(S) = CS^k, \quad (1)$$

was proposed by Twomey (1959b) assuming Junge Power Law Distribution and uniform aerosol chemical composition. This equation contains only two parameters  $C$  and  $k$ . The parameter  $C$  represents the CCN number concentration at supersaturation of 1 %, which is higher in continental and polluted regions than oceanic and clean regions. The parameter  $k$  varies more significantly (Martins et al., 2009). Nevertheless, this equation does not fit CCN spectra well. Ji and Shaw (1998) suggested another formula with three parameters  $N$ ,  $B$  and  $k$ ,

$$N_{\text{CCN}}(S) = N(1 - \exp(-BS^k)), \quad (2)$$

which gave the best fitting among several formulae in Mircea et al. (2005).

Measured CCN spectra in Wuqing were fitted using the two formulae. The probability distribution functions for the fitting parameters were shown in Figs. 1a and 2a. All five fitted parameters varied in wide ranges, indicating that it was improper to represent the CCN spectra using constant parameters in models.

The parameters  $C$  and  $N$  correlated well with the aerosol number concentration (Figs. 1b and 2b), while simple relationships between other parameters and aerosol properties were not found.  $C$  and  $N$  could thereby be predicted assuming a linear relationship with aerosol number concentrations (diameter larger than 50 nm)  $N_{\text{CN}, > 50 \text{ nm}}$ , with other parameters set as the averages during the whole campaign. CCN number concentrations were then calculated using the

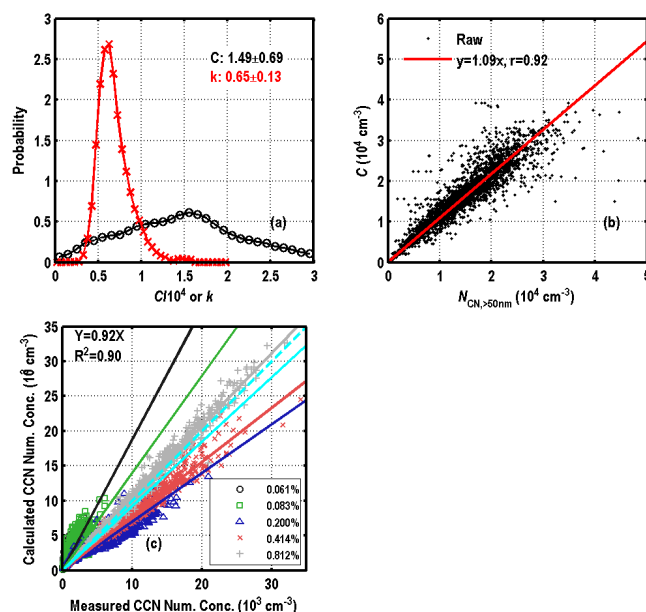


**Fig. 1.** (a) PDF of fitting parameters. The numbers are average values and corresponding standard deviation. (b) Linear relationship between aerosol (larger than 50 nm) number concentration and fitting parameter  $C$ . (c) Prediction of CCN number concentration. The scattered data are the pairs of measurement and calculation, with one colour for each supersaturation. The linearly fitted lines are shown with corresponding colours. The cyan beeline is a linear fitted line for all the data. The cyan dashed line is a 1:1 line.

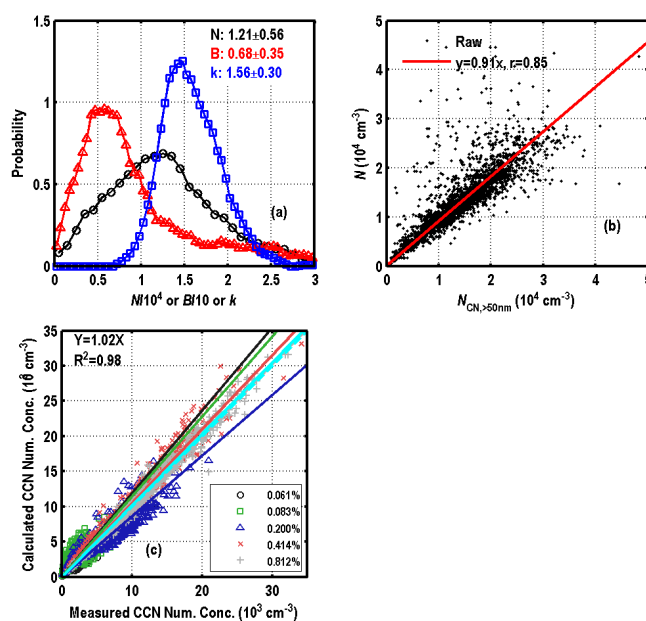


**Fig. 2.** Fitted results of  $N_{\text{CCN}} = N(1 - \exp(-BS^k))$  and comparison of measured CCN number concentrations to calculated ones using CCN spectra parameterization.

two formulas. Calculated CCN number concentrations correlated well with measurements at high supersaturations, but less correlated at low supersaturations (Figs. 1c and 2c). The slopes of fitted lines between measurements and calculations were far from 1 (0.7 to 1.7) if the CCN spectra were expressed as formula (1). CCN spectra could not be well represented at low supersaturations even if the parameters vary with the aerosol number concentration. Formula (1) was only capable of predicting CCN number concentrations at supersaturations around 1%. Formula (2) did not show a systematic estimation bias at either high or low supersaturations. The prediction of the CCN number concentration using either formula correlated poorly with measurements at low supersaturations.

### 3.2 Calculation of CCN number concentrations using bulk activation ratios

Empirical parameterization of CCN spectra failed mainly because CCN spectra cannot be accurately fitted by formulas. Since CCN number concentrations were largely controlled by the population of aerosol particles, we tried to improve CCN predictions by relating CCN number concentrations to aerosol number concentrations. A bulk activation ratio ( $A_{\text{Bulk}}$ ) is often used to characterise this relationship, i.e.  $A_{\text{Bulk}}(S) = N_{\text{CCN,m}}(S)/N_{\text{Ref}}$ , where  $N_{\text{CCN,m}}(S)$  is the measured CCN number concentration at supersaturation  $S$ . The reference aerosol number concentration  $N_{\text{Ref}}$  usually represents the measured number concentration of particles within the measured size range. Since the measured aerosol size range might differ in each campaign, bulk activation ratios derived from  $N_{\text{Ref}}$  may not be directly comparable. The bulk activation ratios in this study were obtained using different reference aerosol number concentrations and applied to CCN calculations. Three reference aerosol number concentrations were considered below, namely, (1) total aerosol number concentrations, (2) accumulation mode aerosol number concentrations, and (3) CCN number concentrations assuming ammonium sulfate aerosol.

#### 3.2.1 Using ratios between measured CCN number concentrations and total aerosol number concentrations

Bulk activation ratios derived using the total aerosol number concentration (here we used the number concentration of particles with diameter larger than 10 nm,  $N_{\text{CN,>10nm}}$ ) ( $A_{\text{Bulk,Tot}} = N_{\text{CCN,m}}(S)/N_{\text{CN,>10nm}}$ ) were often reported in literatures. Pruppacher and Klett (1997) summarised previous measurements and indicated that  $A_{\text{Bulk,Tot}}$  (1% supersaturation ratio) were in the range of 0.2–0.6 for maritime aerosols and 0.004–0.25 for continental aerosols. Bulk activation ratios measured in the Amazon Basin, however, averaged 0.070, 0.235, 0.458, 0.682 and 0.818 at supersaturations of 0.15, 0.30, 0.60, 1.00 and 1.5%, respectively (Roberts et

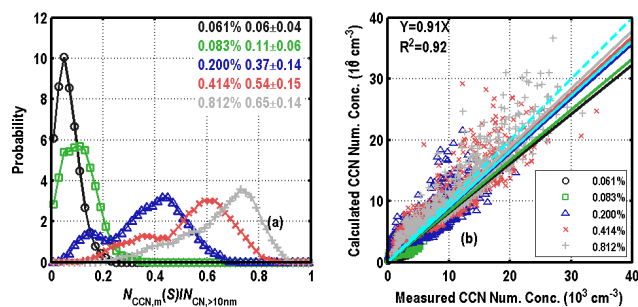


**Fig. 3.** (a) PDF of fitting parameters; (b) Linear relationship between aerosol (larger than 50 nm) number concentration and fitting parameter  $N$ ; (c): Prediction of CCN number concentration.

al., 2002). Bulk activation ratios (based on  $N_{\text{CN,3–900nm}}$ ) measured near the megacity of Guangzhou in China averaged 0.06, 0.36, 0.53, 0.59, 0.71 and 0.85 at supersaturations of 0.068, 0.27, 0.47, 0.67, 0.87 and 1.27%, respectively (Rose et al., 2010). The average bulk activation ratios (based on  $N_{\text{CN,10–460nm}}$ ) measured in east Mediterranean were approximately 0.5, 0.7 and 0.8 at supersaturations of 0.21, 0.38 and above 0.5%, respectively (Bougiatioti et al., 2009).

Figure 3a shows the probability distribution functions (PDF) of bulk activation ratios  $A_{\text{Bulk,Tot}}$  at different supersaturations in Wuqing. The reference number concentration is the total aerosol number concentration within the measured size range of 10 nm–10  $\mu\text{m}$ . Bulk activation ratios at 0.061 and 0.083% mostly range from nearly 0 to 0.2. Bulk activation ratios at supersaturations above 0.200% show a large variation, which are probably attributed to the variation of aerosol particle sizes, i.e. the shape of PNSD. Since size-resolved activation ratios were relatively stable, bulk activation ratios were large when the fraction of particles larger than  $D_{50}$  (see Sect. 3.4.1) was large and vice versa.

Here we examined the results of using this ratio to predict CCN number concentrations. Average bulk activation ratios were 0.06, 0.11, 0.37, 0.54 and 0.65 at supersaturations of 0.061, 0.083, 0.200, 0.414 and 0.812%, respectively. CCN number concentrations were calculated by multiplying total aerosol number concentrations with average bulk activation ratios. The results are shown in Fig. 3b and the slopes of fitted lines and correlation coefficients are listed in Table 2. The correlation coefficients of measured and calculated CCN number concentrations at each supersaturation were mostly below 0.8, with lower values for lower supersaturations. The reference aerosol number concentration counted in particles that would never be activated at any atmospheric cloud supersaturations, i.e. particles with a diameter of 10–30 nm, within which the number of particles could be either small (accumulation mode dominant conditions) or large (new particle formation events). Although these particles were too small to contribute to aerosol activation, they have a large impact on the bulk activation ratio. Therefore, it is not a proper method to calculate CCN number concentrations using bulk

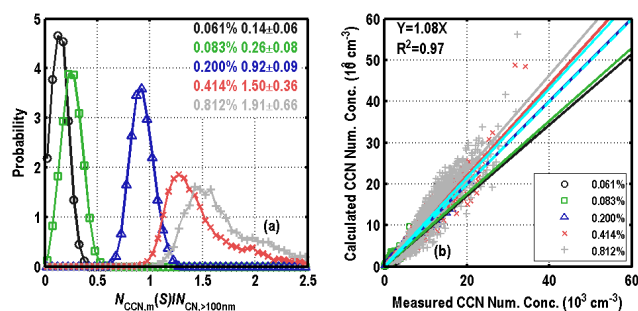


**Fig. 4.** (a) PDF of accumulation mode number based bulk activation ratio  $N_{CCN,m}(S)/N_{CN,>100nm}$  and (b) comparison of measured CCN number concentrations to calculated concentrations using mean  $N_{CCN,m}(S)/N_{CN,>100nm}$ .

activation ratios derived from the total aerosol number concentration, especially for low supersaturation conditions.

### 3.2.2 Using ratios between measured CCN number concentrations and accumulative mode aerosol number concentrations

Bulk activation ratios can also be obtained using measurements of CCN and accumulation mode aerosols. The PNSD of accumulation mode (with diameter larger than 100 nm) aerosols is usually measured by airborne optical particle counters (OPC), such as the passive cavity aerosol spectrometer probe (PCASP). Bulk activation ratios derived from PCASP number concentrations ranged 0.41 to 0.85 at supersaturations of 0.36 % for the dry season and 0.20 to 0.45 at supersaturation of 0.28 % for the wet season over southern Africa (Ross et al., 2003). Breed et al. (2002) found bulk activation ratios less than 1 within the boundary layer and larger than 1 above the boundary layer.

Bulk activation ratios derived from the accumulation mode aerosol number concentration ( $N_{CN,>100nm}$ ) ( $A_{Bulk,Acc} = N_{CCN,m}(S)/N_{CN,>100nm}$ ) in Wuqing were presented in Fig. 4a.  $A_{Bulk,Acc}$  were well below 1 at supersaturations of 0.061 and 0.083 %.  $A_{Bulk,Acc}$  at 0.200 % were around 1, because CCN at this supersaturation mainly consist of particles larger than 100 nm. Particles smaller than 100 nm also contributed to CCN at supersaturations of 0.414 and 0.812 %, resulting in  $A_{Bulk,Acc}$  above 1.

$A_{Bulk,Acc}$  averaged over the campaign were also used to calculate CCN number concentrations (Fig. 4b). Correlation coefficients of measured and calculated CCN number concentrations were larger than 0.60 at all supersaturations, also larger than those in the case of using  $A_{Bulk,Tot}$ . Accumulation mode particles are better indicators of the CCN population than total aerosol particles. The best agreement was achieved at supersaturation of 0.200 %, with the slope of the fitted line close to 1 and the correlation coefficient around 0.95. This can be understood since CCN at a supersaturation of 0.20 % are mostly comprised of those particles larger than a critical

diameter of 100 nm which contain a significant mass fraction of water soluble compounds, e.g. sulfate, nitrate and oxidized organics. At other supersaturations, correlations between measured and calculated CCN number concentrations were not as good as that at supersaturation of 0.200 %. The clear explanation is that at lower and higher supersaturations, the critical diameters are respectively larger or smaller than 100 nm and include a smaller or larger integral of the PNSD. Thus, the measured CCN concentrations at 0.20 %, is best represented by the integral of PNSD concentration greater than 100 nm, i.e. roughly the accumulation mode.

### 3.2.3 Using ammonium sulfate as reference aerosol composition

The applications of  $A_{Bulk,Tot}$  and  $A_{Bulk,Acc}$  showed that it is of great importance to choose appropriate size ranges of the reference number concentration for bulk activation ratios in the calculation of CCN number concentration. A fixed size range might be suitable for one supersaturation but inadequate for others. Therefore, choosing different size ranges of reference number concentrations for different supersaturations might improve the application of bulk activation ratios in calculating CCN number concentrations.

The hygroscopic growth and activation behaviour of ammonium sulfate can be predicted theoretically (Low, 1969; Young and Warren, 1992; Tang and Munkelwitz, 1994), and often used in instrument calibration. Here, we propose a method using ammonium sulfate as a reference substance to represent the overall aerosol activation properties. CCN number concentration ( $N_{CCN,AS}(S)$ ) at supersaturation  $S$  was calculated by integrating the PNSD with diameters greater than the critical diameter of ammonium sulfate at  $S$  (Tabl 1), assuming that all particles were composed of 100 % ammonium sulfate and taken as the reference number concentration. The bulk activation ratio derived from these reference CCN number concentrations ( $A_{Bulk,AS} = N_{CCN,m}(S)/N_{CCN,AS}(S)$ ) roughly represents the fraction of ammonium sulfate in an external mixture with insoluble materials.

The probability distribution of  $A_{Bulk,AS}$  was displayed in Fig. 5a.  $A_{Bulk,AS}$  was above 0.7 at supersaturations of 0.200 % and higher, whereas it was only about 0.4 at lower supersaturations as a result of less soluble materials contained in larger particles. CCN number concentrations were even better predicted by the method using average  $A_{Bulk,AS}$  during the campaign than the two methods introduced in Sects. 3.2.1 and 3.2.2 (Fig. 5b). The slopes of the fitted line were close to 1. The correlation coefficients between calculated and measured CCN number concentrations were 0.84 and 0.86 at supersaturations of 0.061 % and 0.083 %, and above 0.90 at supersaturations of 0.200 % and higher.

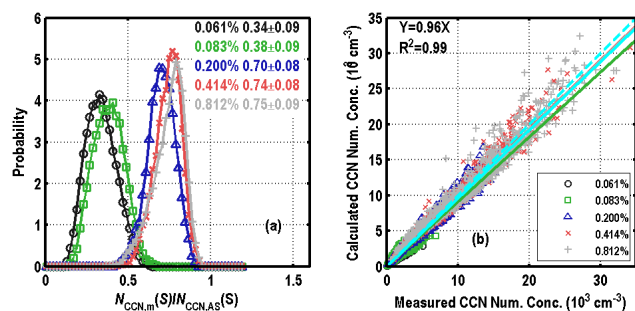


**Fig. 5.** (a) PDF of  $N_{CCN,m}(S)/N_{CCN,AS}(S)$  and (b) comparison of measured CCN number concentrations to calculated ones using mean  $N_{CCN,m}(S)/N_{CCN,AS}(S)$ .

### 3.3 Calculation of CCN number concentrations using inferred critical diameter

The methods presented in the sections above used measurements of CCN and aerosol number concentrations for CCN parameterizations. In addition to the aerosol number concentration, the size of aerosols was another important factor for controlling the CCN number concentration. In this section, the PNSD of aerosols were included to improve the calculation of CCN number concentrations.

With an assumption of uniform, internally mixed but unspecified chemical composition throughout the size range, a critical dry particle diameter ( $D_{inf}$ ) can be inferred from measured CCN number concentrations and PNSD, namely, the integral of PNSD larger than  $D_{inf}$  equals to the measured CCN number concentration. Particles with diameter larger than  $D_{inf}$  can be activated at a given supersaturation, while smaller ones cannot. Results were shown in Fig. 6a. At two lower supersaturations, the probability distribution functions of the inferred critical diameters were comparable to those in Deng et al. (2011). At higher supersaturations, PDF had two peaks in Deng et al. (2011), while only one peak in this study. A wider range of  $D_{inf}$  in last paper corresponded to water depletion in CCNC (Latham and Nenes, 2011). Bulk CCN number concentrations were underestimated when abundant aerosol particles were activated, which would result in overestimated inferred critical diameters.

Average inferred critical diameter for each supersaturation was used as a cut-off diameter to calculate CCN number concentrations (Fig. 6b). Surprisingly, calculated CCN number concentrations matched well with measured ones. The slopes of fitted lines were 0.96, 0.98, 1.00, 1.01 and 1.01 for supersaturations of 0.061, 0.083, 0.200, 0.414 and 0.812 %, respectively. The correlation coefficients were above 0.8 at all supersaturations. These results suggest that the method using inferred critical diameters is capable of easily and precisely predicting CCN number concentrations.

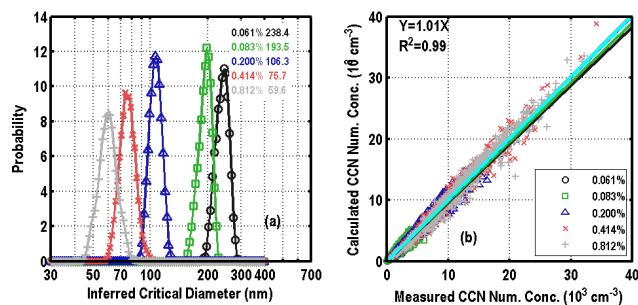


**Fig. 6.** (a) PDF of inferred critical diameters and (b) comparison of measured CCN number concentrations to calculated ones using mean inferred critical diameters.

### 3.4 Calculation of CCN number concentrations using size-resolved activation ratios

Size-resolved activation ratios, combined with PNSD, provide a straightforward way to calculate CCN number concentrations. Size-resolved activation ratios depend on the chemical composition and mixing state of aerosol, which are not usually available through measurements or models. Here several methods for CCN parameterization are examined using measured size-resolved activation ratios.

#### 3.4.1 Using $D_{50}$ derived from activation curves

Size-resolved activation ratios provide another cut-off diameter for CCN calculations. A critical diameter, denoted as  $D_{50}$ , is often derived from measured size-resolved activation ratios.  $D_{50}$  is the diameter at which 50 % of the particles are activated. Multiply charged particles would influence the determination of  $D_{50}$ . If the mode diameter of the polydisperse size distribution exceeds the critical diameter of the particles, multiply charged particles may lead to nonmonotonic CCN counter response curves (Petters et al., 2007). Frank et al. (2006) and Deng et al. (2011) have proposed procedures for the multiple charge correction. Size-resolved activation ratios in this study were inverted to eliminate the effects of multiply charge and DMA transfer function.

$D_{50}$  of a simple sigmoidally shaped activation curve is determined by fitting the size-resolved activation ratios with a formula as seen below,

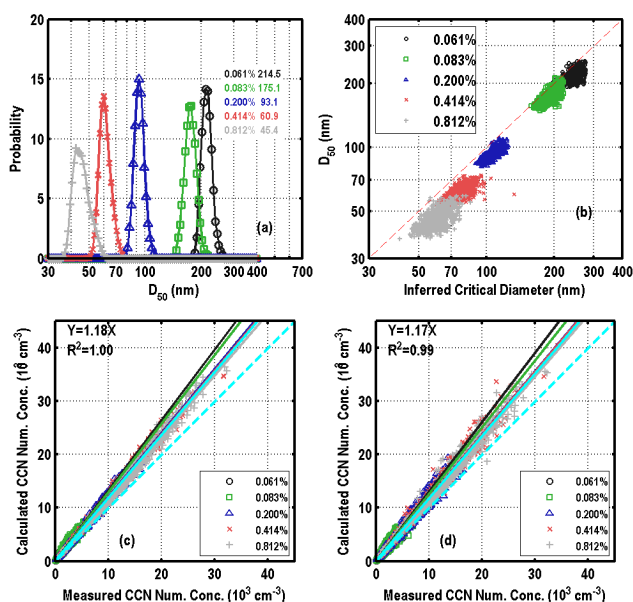
$$A(D_p) = d / \{1 + \exp[(D_{50} - D_p)/a]\}, \quad (3)$$

where  $A(D_p)$  is the activation ratio of particles with diameter  $D_p$ ,  $a$  and  $d$  are fitting constants. The maximum activation ratios  $d$  are not always 1, due to the measurement uncertainty and sometimes insufficient size range. Thus,  $D_{50}$  is usually defined as the diameter at which  $0.5d$  of the aerosol particles are activated.

Figure 7a presents the PDF of  $D_{50}$ . The critical diameters of ambient particles, both  $D_{50}$  and  $D_{inf}$ , were larger than those of ammonium sulfate, and the hygroscopicity parameter  $\kappa$  (with  $\kappa$  from  $D_{50}$  of 0.19–0.39 and  $\kappa$  from  $D_{inf}$  of

**Table 1.** Critical sizes for ammonium sulfate particles ( $D_{C,AS}$ ), as well as the measured  $D_{50}$  and  $D_{inf}$  and corresponding hygroscopicity parameter  $\kappa$ . The measured  $D_{50}$ ,  $D_{inf}$  and  $\kappa$  are reported as mean  $\pm$  standard deviation and minimum  $\sim$  maximum.

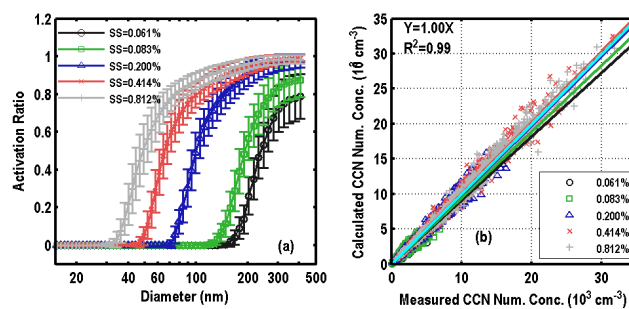
SS	$D_{C,AS}$ (nm)	$D_{50}$ (nm)	$\kappa$ from $D_{50}$	$D_{inf}$ (nm)	$\kappa$ from $D_{inf}$
0.061	175	215 $\pm$ 12; 189–254	0.35 $\pm$ 0.06; 0.20–0.53	238 $\pm$ 17; 193–275	0.26 $\pm$ 0.06; 0.16–0.48
0.083	143	175 $\pm$ 12; 148–212	0.35 $\pm$ 0.07; 0.19–0.56	194 $\pm$ 13; 157–220	0.26 $\pm$ 0.06; 0.17–0.48
0.200	81	93 $\pm$ 5; 81–110	0.39 $\pm$ 0.07; 0.22–0.59	106 $\pm$ 7; 90–125	0.26 $\pm$ 0.06; 0.16–0.46
0.414	49	61 $\pm$ 4; 53–74	0.31 $\pm$ 0.06; 0.18–0.49	76 $\pm$ 7; 60–133	0.17 $\pm$ 0.05; 0.03–0.34
0.812	31	45 $\pm$ 4; 37–59	0.19 $\pm$ 0.05; 0.08–0.33	60 $\pm$ 7; 41–85	0.08 $\pm$ 0.03; 0.03–0.24

**Fig. 7.**  $D_{50}$  and the application of mean  $D_{50}$  to calculation of CCN number concentrations.

0.08–0.26) was smaller (Table 1), suggesting that the hygroscopicity of ambient particles was lower than ammonium sulfate. The average  $D_{50}$ , namely 214.5, 175.1, 93.1, 60.9 and 45.4 nm at each supersaturation, were lower than the inferred critical dry diameter (Fig. 7b). There are three possible reasons for such a difference.

First, the activation curves were not sigmoidally shaped. The activation curve measured in the NCP, in both this study (Fig. 8a) and Deng et al. (2011), were not ideal sigmoidally shaped. Measured activation ratios were lower than what a sigmoidal function would give at the diameters where activation ratios were close to the maximum. Similar activation curves were also found in Beijing (Gunthe et al., 2011). Such non-sigmoidally shaped activation curves resulted from the externally mixed aerosols. Assuming a flat PNSD ( $dN/d\log D_p$  is constant), lower activation ratios at diameters above  $D_{50}$  due to less hygroscopic particles would lead to  $D_{inf} > D_{50}$ .

Second, the PNSD were not flat. If  $D_{50}$  was smaller than the peak diameter (in the case of higher supersaturations),

**Fig. 8.** (a) Average size-resolved activation ratios and (b) comparison of measured CCN number concentrations to calculated ones using average size-resolved activation ratios.

$D_{inf} > D_{50}$ , while  $D_{inf} < D_{50}$  if  $D_{50}$  was larger than the peak diameter (in the case of lower supersaturations).

Third,  $D_{inf}$  might be larger than  $D_{50}$ , when the maximum activation ratios were lower than 1 for the reason of the measurement uncertainty and insufficient measuring range.

Using  $D_{50}$  (either real-time or campaign average) to calculate CCN number concentrations resulted in an overestimation of about 20 % (Fig. 7c and d). Based on these results, predictions of the CCN number concentration might be biased due to the improper determination of  $D_{50}$  for externally mixed aerosol.

### 3.4.2 Using averaged activation curves without diurnal variation

Similar to the inferred critical diameter,  $D_{50}$  was derived assuming a uniform aerosol chemical composition. However, aerosols in the North China Plain were found to be usually externally mixed (Liu et al., 2011). Size-resolved activation ratios, which contain information on aerosol mixing states, are hopeful in the improvement of the CCN calculations.

Average size-resolved activation ratios during the campaign were shown in Fig. 8a. To test how well the average condition represented size-resolved activation properties of aerosols, the temporal variations of the activation curves were not considered. CCN number concentrations calculated using measured PNSD and average size-resolved activation ratios are shown in Fig. 8b. Measured and calculated CCN number concentrations were linearly fitted. The slopes of the

**Table 2.** Slope and  $R^2$  values are averages over all supersaturations. Numbers in parentheses are ranges of slopes and  $R^2$  at specific supersaturations.

Category	Principle	Details	$R^2$	Slope
CCN spectra	The parameters in the formula are expressed as a function of $N_{\text{CN}}(D > 50 \text{ nm})$	$N_{\text{CCN}} = \text{CS}^k$	0.90 (0.47–0.99)	0.92 (0.70–1.88)
		$N_{\text{CCN}} = N_0(1 - \exp(-BS^k))$	0.98 (0.46–0.99)	1.02 (0.86–1.18)
Bulk activation ratio $A_{\text{Bulk}} = N_{\text{CCN}}/N_{\text{Ref}}$	$N_{\text{CN}}^* A_{\text{Bulk, Mean}}$	$N_{\text{Ref}} = N_{\text{CN}, > 10 \text{ nm}}$	0.92 (0.31–0.87)	0.91 (0.81–0.95)
		$N_{\text{Ref}} = N_{\text{CN}, > 100 \text{ nm}}$	0.97 (0.70–0.97)	1.08 (0.86–1.16)
		$N_{\text{Ref}} = N_{\text{CCN, AS}}(S)$	0.99 (0.84–0.97)	0.96 (0.91–0.97)
Cut-off diameter	Use a cut-off diameter to distinguish CCN-active and CCN-inactive particles	Critical dry diameter $D_{\text{inf}}$ is inferred from the measured PNSD and $N_{\text{CCN, m}}$ . Campaign average $D_{\text{inf}}$ is used.	0.99 (0.88–0.98)	1.01 (0.96–1.01)
		$D_{50}$ , Real-time	1.00 (0.93–0.99)	1.18 (1.16–1.32)
		$D_{50}$ , Campaign Average	0.99 (0.87–0.99)	1.17 (1.16–1.30)
Size-resolved activation ratios	$n_{\text{CN}}(D_p) \cdot A(D_p)$ $n_{\text{CN}}(D_p) \cdot A(D_p) \rightarrow n_{\text{CCN}}(D_p) \rightarrow N_{\text{CCN}}$	Campaign average of the activation curves	0.99 (0.88–0.99)	1.00 (0.94–1.00)
		Diurnal variation of the activation curves	0.99 (0.90–0.99)	0.99 (0.95–1.00)

fitted lines and the correlation coefficients at different supersaturations are given in Table 2. The calculation slightly underestimates CCN number concentrations, and the correlation coefficients were below 0.9 at supersaturations of 0.061 and 0.083 %, at which size-resolved activation ratios display a larger variability than those at higher supersaturations. The slopes of the fitted lines are close to 1 and the correlation coefficients are above 0.95 at supersaturations of 0.200 % and higher. The method using average size-resolved activation ratios to calculate CCN number concentrations generally provides a reasonable estimation.

### 3.4.3 Using averaged activation curves with diurnal variation

Size-resolved activation ratios had strong diurnal variations at lower supersaturations (Fig. 9a). Emissions in rush hours increased the amount of particles with low hygroscopicity and resulted in lower activation ratios. The increase of activation ratios in daytime was due to aerosol aging. The maximum activation ratios within the measured size range varied significantly at low supersaturations, e.g. 0.7–0.9 and

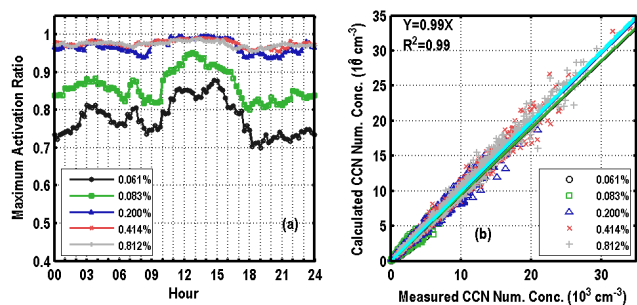
0.75–1.0 at supersaturations of 0.061 and 0.083 %. However,  $D_{50}$  did not show such a large variability.

Figure 9b displays the CCN number concentrations calculated taking into account the diurnal variation of size-resolved activation ratios. The slopes of the fitted lines were similar to those calculated without considering the diurnal variation of size-resolved activation ratios, whereas the correlation coefficients were a little higher.

## 4 Summary and conclusion

In this paper, methods for calculating CCN number concentrations based on aerosol size distributions (summarised in Table 2) were examined using a dataset from HaChi field campaign in the North China Plain. Table 1 shows the slopes of the linear regression (with intercept of 0) and the correlation coefficients ( $R^2$ ) between calculated and measured CCN number concentrations. Slope and  $R^2$  values are the averages over all supersaturations. The numbers in parentheses are the ranges of slopes and  $R^2$  at specific supersaturations.

The method using CCN spectra to predict the CCN number concentration is easily used in models. However, the



**Fig. 9.** (a) Diurnal variation of maximum of size-resolved activation ratios and (b) comparison of measured CCN number concentrations to calculated concentrations using diurnally variant size-resolved activation ratios.

parameters in fitted functions for CCN spectra span over a wide range. Reasonable results of CCN spectra could only be obtained using the number concentration of aerosols with diameters larger than 50 nm at high supersaturations. There is an inevitable limitation of using this method for CCN predictions under very clean and polluted conditions, since aerosol size distributions and chemical compositions are not properly accounted for in this method.

The method using bulk activation ratios together with the aerosol number concentration provides a simple way to calculate the CCN number concentration. Results showed that the ratio between measured CCN number concentrations and total/accumulation mode aerosol number concentrations significantly varied. Assuming externally mixed aerosols of ammonium sulfate and CCN-inactive substances, a new parameterization of CCN number concentration is proposed using bulk activation ratio based on the activated number concentration of ammonium sulfate. The prediction of CCN number concentration using ammonium sulfate-based bulk activation ratio is better than that of total aerosol number concentration-based bulk activation ratio.

The cut-off diameter divides particles into a CCN-active group and a CCN-inactive group.  $D_{50}$  is often obtained from size resolved activation ratios and applied in the calculation of the CCN number concentration. Calculated CCN number concentrations were generally overestimated by about 15–20 % because of the non-sigmoidally shaped activation curves and the non-flat PNSD. Inferred critical dry diameters were inversely calculated, assuming a homogeneous chemical composition. CCN number concentrations can be well predicted using campaign-averaged inferred critical dry diameters at each supersaturation.

Using the above methods, aerosol chemical compositions and mixing states should be assumed. However, ambient aerosols have size-dependent compositions and are often partially externally mixed. The aerosol activation curve contains information on aerosol chemical compositions and mixing states, and could thereby be used to reasonably predict CCN number concentrations on the basis of PNSD. Re-

sults showed that the campaign-averaged activation curves could well-predict CCN number concentrations. Moreover, the agreement between calculated and measured CCN number concentrations was even better when the diurnal variation of size-resolve activation ratios was taken into account.

Based on the criteria that the correlation coefficients of calculated and measured CCN number concentrations are above 0.8 and the fitted slopes between 0.9–1.1, it is recommended that the CCN number concentration be predicted using PNSD together with inferred critical diameters or size-resolved activation ratios.

*Acknowledgements.* This work is supported by the National 973 Project of China (2011CB403402), and the National Natural Science Foundation of China (NSFC) under grants 41205098 and 41005007. This work is also supported by the Meteorology Foundation GYHY200906025, GYHY201006011 and the “Strategic Priority Research Program” of the Chinese Academy of Sciences (XDA05100000).hack

Edited by: D. Covert

## References

- Albrecht, B. A.: Aerosols, Cloud Microphysics, and Fractional Cloudiness, *Science*, 245, 1227–1230, doi:10.1126/science.245.4923.1227, 1989.
- Bigg, E. K., and Leek, C.: Cloud-active particles over the central Arctic Ocean, *J. Geophys. Res.*, 106, 32155–32166, doi:10.1029/1999jd901152, 2001.
- Bougiatioti, A., Fountoukis, C., Kalivitis, N., Pandis, S. N., Nenes, A., and Mihalopoulos, N.: Cloud condensation nuclei measurements in the marine boundary layer of the Eastern Mediterranean: CCN closure and droplet growth kinetics, *Atmos. Chem. Phys.*, 9, 7053–7066, doi:10.5194/acp-9-7053-2009, 2009.
- Breed, D., Brientjes, R., Jensen, T., Salazar, V., and Piketh, S.: Aerosol and cloud droplet measurements in the United Arab Emirates, 11th Conference on Cloud Physics, 2002.
- Delene, D. J. and Deshler, T.: Vertical profiles of cloud condensation nuclei above Wyoming, *J. Geophys. Res.*, 106, 12579–12588, doi:10.1029/2000jd900800, 2001.
- Deng, Z., Zhao, C., Zhang, Q., Huang, M., and Ma, X.: Statistical analysis of microphysical properties and the parameterization of effective radius of warm clouds in Beijing area, *Atmos. Res.*, 93, 888–896, 2009.
- Deng, Z. Z., Zhao, C. S., Ma, N., Liu, P. F., Ran, L., Xu, W. Y., Chen, J., Liang, Z., Liang, S., Huang, M. Y., Ma, X. C., Zhang, Q., Quan, J. N., Yan, P., Henning, S., Mildenberger, K., Sommerhage, E., Schäfer, M., Stratmann, F., and Wiedensohler, A.: Size-resolved and bulk activation properties of aerosols in the North China Plain, *Atmos. Chem. Phys.*, 11, 3835–3846, doi:10.5194/acp-11-3835-2011, 2011.
- Detwiler, A., Langerud, D., and Depue, T.: Investigation of the Variability of Cloud Condensation Nuclei Concentrations at the Surface in Western North Dakota, *J. Appl. Meteorol. Clim.*, 49, 136–145, 2010.

- Dusek, U., Frank, G. P., Hildebrandt, L., Curtius, J., Schneider, J., Walter, S., Chand, D., Drewnick, F., Hings, S., Jung, D., Borrmann, S., and Andreae, M. O.: Size Matters More Than Chemistry for Cloud-Nucleating Ability of Aerosol Particles, *Science*, 312, 1375–1378, doi:10.1126/science.1125261, 2006.
- Ervens, B., Cubison, M. J., Andrews, E., Feingold, G., Ogren, J. A., Jimenez, J. L., Quinn, P. K., Bates, T. S., Wang, J., Zhang, Q., Coe, H., Flynn, M., and Allan, J. D.: CCN predictions using simplified assumptions of organic aerosol composition and mixing state: a synthesis from six different locations, *Atmos. Chem. Phys.*, 10, 4795–4807, doi:10.5194/acp-10-4795-2010, 2010.
- Fitzgerald, J. W.: Dependence of the supersaturation spectrum of CCN on aerosol size distribution and composition, *J. Atmos. Sci.*, 30, 628–634, 1973.
- Frank, G. P., Dusek, U., and Andreae, M. O.: Technical note: A method for measuring size-resolved CCN in the atmosphere, *Atmos. Chem. Phys. Discuss.*, 6, 4879–4895, doi:10.5194/acpd-6-4879-2006, 2006.
- Gunthe, S. S., Rose, D., Su, H., Garland, R. M., Achtert, P., Nowak, A., Wiedensohler, A., Kuwata, M., Takegawa, N., Kondo, Y., Hu, M., Shao, M., Zhu, T., Andreae, M. O., and Pöschl, U.: Cloud condensation nuclei (CCN) from fresh and aged air pollution in the megacity region of Beijing, *Atmos. Chem. Phys.*, 11, 11023–11039, doi:10.5194/acp-11-11023-2011, 2011.
- Hagen, D. E. and Alofs, D. J.: Linear Inversion Method to Obtain Aerosol Size Distributions from Measurements with a Differential Mobility Analyzer, *Aerosol Sci. Tech.*, 2, 465–475, 1983.
- Hobbs, P. V., Stith, J. L., and Radke, L. F.: Cloud-Active Nuclei from Coal-Fired Electric Power Plants and Their Interactions with Clouds, *J. Appl. Meteorol.*, 19, 439–451, doi:10.1175/1520-0450(1980)019<0439:canfcf>2.0.CO;2, 1980.
- Hudson, J. G. and Yum, S. S.: Cloud condensation nuclei spectra and polluted and clean clouds over the Indian Ocean, *J. Geophys. Res.*, 107, 8022, doi:10.1029/2001jd000829, 2002.
- Hudson, J. G., Garrett, T. J., Hobbs, P. V., Strader, S. R., Xie, Y., and Yum, S. S.: Cloud Condensation Nuclei and Ship Tracks, *J. Atmos. Sci.*, 57, 2696–2706, doi:10.1175/1520-0469(2000)057<2696:CCNAST>2.0.CO;2, 2000.
- Ji, Q. and Shaw, G. E.: On supersaturation spectrum and size distributions of cloud condensation nuclei, *Geophys. Res. Lett.*, 25, 1903–1906, doi:10.1029/98gl01404, 1998.
- Junge, C. and McLaren, E.: Relationship of cloud nuclei spectra to aerosol size distribution and composition, *J. Atmos. Sci.*, 28, 382–390, 1971.
- Kammermann, L., Gysel, M., Weingartner, E., Herich, H., Cziczó, D. J., Holst, T., Svenningsson, B., Arneth, A., and Baltensperger, U.: Subarctic atmospheric aerosol composition: 3. Measured and modeled properties of cloud condensation nuclei, *J. Geophys. Res.*, 115, D04202, doi:10.1029/2009jd012447, 2010.
- Kerminen, V.-M., Paramonov, M., Anttila, T., Riipinen, I., Fountoukis, C., Korhonen, H., Asmi, E., Laakso, L., Lihavainen, H., Swietlicki, E., Svenningsson, B., Asmi, A., Pandis, S. N., Kulmala, M., and Petäjä, T.: Cloud condensation nuclei production associated with atmospheric nucleation: a synthesis based on existing literature and new results, *Atmos. Chem. Phys.*, 12, 12037–12059, doi:10.5194/acp-12-12037-2012, 2012.
- Knutson, E. O. and Whitby, K. T.: Aerosol classification by electric mobility: apparatus, theory, and applications, *J. Aerosol Sci.*, 6, 443–451, 1975.
- Kuwata, M., Kondo, Y., Miyazaki, Y., Komazaki, Y., Kim, J. H., Yum, S. S., Tanimoto, H., and Matsueda, H.: Cloud condensation nuclei activity at Jeju Island, Korea in spring 2005, *Atmos. Chem. Phys.*, 8, 2933–2948, doi:10.5194/acp-8-2933-2008, 2008.
- Lance, S., Medina, J., Smith, J. N., and Nenes, A.: Mapping the operation of the DMT continuous flow CCN counter, *Aerosol Sci. Technol.*, 40, 242–254, 2006.
- Latham, T. L. and Nenes, A.: Water Vapor Depletion in the DMT Continuous-Flow CCN Chamber: Effects on Supersaturation and Droplet Growth, *Aerosol Sci. Tech.*, 45, 604–615, doi:10.1080/02786826.2010.551146, 2011.
- Liu, P. F., Zhao, C. S., Göbel, T., Hallbauer, E., Nowak, A., Ran, L., Xu, W. Y., Deng, Z. Z., Ma, N., Mildenberger, K., Henning, S., Stratmann, F., and Wiedensohler, A.: Hygroscopic properties of aerosol particles at high relative humidity and their diurnal variations in the North China Plain, *Atmos. Chem. Phys.*, 11, 3479–3494, doi:10.5194/acp-11-3479-2011, 2011.
- Low, R. D. H.: A generalized equation for the solution effect in droplet growth, *J. Atmos. Sci.*, 26, 608–611, 1969.
- Ma, N., Zhao, C. S., Nowak, A., Müller, T., Pfeifer, S., Cheng, Y. F., Deng, Z. Z., Liu, P. F., Xu, W. Y., Ran, L., Yan, P., Göbel, T., Hallbauer, E., Mildenberger, K., Henning, S., Yu, J., Chen, L. L., Zhou, X. J., Stratmann, F., and Wiedensohler, A.: Aerosol optical properties in the North China Plain during HaChi campaign: an in-situ optical closure study, *Atmos. Chem. Phys.*, 11, 5959–5973, doi:10.5194/acp-11-5959-2011, 2011.
- Ma, N., Zhao, C. S., Müller, T., Cheng, Y. F., Liu, P. F., Deng, Z. Z., Xu, W. Y., Ran, L., Nekat, B., van Pinxteren, D., Gnauk, T., Müller, K., Herrmann, H., Yan, P., Zhou, X. J., and Wiedensohler, A.: A new method to determine the mixing state of light absorbing carbonaceous using the measured aerosol optical properties and number size distributions, *Atmos. Chem. Phys.*, 12, 2381–2397, doi:10.5194/acp-12-2381-2012, 2012.
- Martins, J., Gonçalves, F., Morales, C., Fisch, G., Pinheiro, F., Leal Júnior, J., Oliveira, C., Silva, E., Oliveira, J., Costa, A., and Silva Dias, M.: Cloud condensation nuclei from biomass burning during the Amazonian dry-to-wet transition season, *Meteorol. Atmos. Phys.*, 104, 83–93, 2009.
- Medina, J., Nenes, A., Sotiropoulou, R.-E. P., Cottrell, L. D., Ziemba, L. D., Beckman, P. J., and Griffin, R. J.: Cloud condensation nuclei closure during the International Consortium for Atmospheric Research on Transport and Transformation 2004 campaign: Effects of size-resolved composition, *J. Geophys. Res.*, 112, D10S31, doi:10.1029/2006jd007588, 2007.
- Mircea, M., Facchini, M. C., Decesari, S., Cavalli, F., Emblico, L., Fuzzi, S., Vestin, A., Rissler, J., Swietlicki, E., Frank, G., Andreae, M. O., Maenhaut, W., Rudich, Y., and Artaxo, P.: Importance of the organic aerosol fraction for modeling aerosol hygroscopic growth and activation: a case study in the Amazon Basin, *Atmos. Chem. Phys.*, 5, 3111–3126, doi:10.5194/acp-5-3111-2005, 2005.
- Moore, R. H., Nenes, A., and Medina, J.: Scanning mobility CCN analysis—a method for fast measurements of size-resolved CCN distributions and activation kinetics, *Aerosol Sci. Tech.*, 44, 861–871, 2010.
- Petters, M. D., Prenni, A. J., Kreidenweis, S. M., and DeMott, P. J.: On Measuring the Critical Diameter of Cloud Condensation

- Nuclei Using Mobility Selected Aerosol, *Aerosol Sci. Tech.*, 41, 907–913, 2007.
- Pruppacher, H. R. and Klett, J. D.: Microphysics of clouds and precipitation, Kluwer Academic Publishers, Dordrecht, the Netherlands, 944 pp., 1997.
- Ramanathan, V., Crutzen, P. J., Kiehl, J. T., and Rosenfeld, D.: Aerosols, Climate, and the Hydrological Cycle, *Science*, 294, 2119–2124, doi:10.1126/science.1064034, 2001.
- Ran, L., Zhao, C. S., Xu, W. Y., Lu, X. Q., Han, M., Lin, W. L., Yan, P., Xu, X. B., Deng, Z. Z., Ma, N., Liu, P. F., Yu, J., Liang, W. D., and Chen, L. L.: VOC reactivity and its effect on ozone production during the HaChi summer campaign, *Atmos. Chem. Phys.*, 11, 4657–4667, doi:10.5194/acp-11-4657-2011, 2011.
- Roberts, G. C. and Nenes, A.: A continuous-flow streamwise thermal-gradient CCN chamber for atmospheric measurements, *Aerosol Sci. Tech.*, 39, 206–221, 2005.
- Roberts, G. C., Artaxo, P., Zhou, J., Swietlicki, E., and Andreae, M. O.: Sensitivity of CCN spectra on chemical and physical properties of aerosol: A case study from the Amazon Basin, *J. Geophys. Res.*, 107, 8070, doi:10.1029/2001jd000583, 2002.
- Rose, D., Gunthe, S. S., Mikhailov, E., Frank, G. P., Dusek, U., Andreae, M. O., and Pöschl, U.: Calibration and measurement uncertainties of a continuous-flow cloud condensation nuclei counter (DMT-CCNC): CCN activation of ammonium sulfate and sodium chloride aerosol particles in theory and experiment, *Atmos. Chem. Phys.*, 8, 1153–1179, doi:10.5194/acp-8-1153-2008, 2008.
- Rose, D., Nowak, A., Achtert, P., Wiedensohler, A., Hu, M., Shao, M., Zhang, Y., Andreae, M. O., and Pöschl, U.: Cloud condensation nuclei in polluted air and biomass burning smoke near the mega-city Guangzhou, China – Part 1: Size-resolved measurements and implications for the modeling of aerosol particle hygroscopicity and CCN activity, *Atmos. Chem. Phys.*, 10, 3365–3383, doi:10.5194/acp-10-3365-2010, 2010.
- Ross, K. E., Pikh, S. J., Bruintjes, R. T., Burger, R. P., Swap, R. J., and Annegarn, H. J.: Spatial and seasonal variations in CCN distribution and the aerosol-CCN relationship over southern Africa, *J. Geophys. Res.*, 108, 8481, doi:10.1029/2002jd002384, 2003.
- Snider, J. R. and Brenguier, J. L.: Cloud condensation nuclei and cloud droplet measurements during ACE-2, *Tellus B*, 52, 828–842, 2000.
- Squires, P. and Twomey, S.: A Comparison of Cloud Nucleus Measurements over Central North America and the Caribbean Sea, *J. Atmos. Sci.*, 23, 401–404, doi:10.1175/1520-0469(1966)023<0401:acocnm>2.0.CO;2, 1966.
- Stroud, C. A., Nenes, A., Jimenez, J. L., DeCarlo, P. F., Huffman, J. A., Bruintjes, R., Nemitz, E., Delia, A. E., Toohey, D. W., Guenther, A. B., and Nandi, S.: Cloud Activating Properties of Aerosol Observed during CELTIC, *J. Atmos. Sci.*, 64, 441–459, 2007.
- Tang, I. N. and Munkelwitz, H. R.: Water activities, densities, and refractive indices of aqueous sulfates and sodium nitrate droplets of atmospheric importance, *J. Geophys. Res.*, 99, 801–808, 1994.
- Twohy, C. H. and Anderson, J. R.: Droplet nuclei in non-precipitating clouds: composition and size matter, *Environ. Res. Lett.*, 3, 045002, doi:10.1088/1748-9326/3/4/045002, 2008.
- Twomey, S.: The nuclei of natural cloud formation part I: The chemical diffusion method and its application to atmospheric nuclei, *Pure Appl. Geophys.*, 43, 227–242, 1959a.
- Twomey, S.: The nuclei of natural cloud formation part II: The supersaturation in natural clouds and the variation of cloud droplet concentration, *Pure Appl. Geophys.*, 43, 243–249, 1959b.
- Twomey, S.: Pollution and the Planetary Albedo, *Atmos. Environ.*, 8, 1251–1256, 1974.
- Twomey, S. and Warner, J.: Comparison of Measurements of Cloud Droplets and Cloud Nuclei, *J. Atmos. Sci.*, 24, 702–703, doi:10.1175/1520-0469(1967)024<0702:COMOCD>2.0.CO;2, 1967.
- Wang, J., Cubison, M. J., Aiken, A. C., Jimenez, J. L., and Collins, D. R.: The importance of aerosol mixing state and size-resolved composition on CCN concentration and the variation of the importance with atmospheric aging of aerosols, *Atmos. Chem. Phys.*, 10, 7267–7283, doi:10.5194/acp-10-7267-2010, 2010.
- Wex, H., McFiggans, G., Henning, S., and Stratmann, F.: Influence of the external mixing state of atmospheric aerosol on derived CCN number concentrations, *Geophys. Res. Lett.*, 37, 10805, doi:10.1029/2010GL043337, 2010.
- Wiedensohler, A.: An approximation of the bipolar charge distribution for particles in the submicron size range, *J. Aerosol Sci.*, 19, 387–389, 1988.
- Wiedensohler, A., Birmili, W., Nowak, A., Sonntag, A., Weinhold, K., Merkel, M., Wehner, B., Tuch, T., Pfeifer, S., Fiebig, M., Fjåraa, A. M., Asmi, E., Sellegri, K., Depuy, R., Venzac, H., Villani, P., Laj, P., Aalto, P., Ogren, J. A., Swietlicki, E., Williams, P., Roldin, P., Quincey, P., Hüglin, C., Fierz-Schmidhauser, R., Gysel, M., Weingartner, E., Riccobono, F., Santos, S., Gröning, C., Faloon, K., Beddows, D., Harrison, R., Monahan, C., Jennings, S. G., O’Dowd, C. D., Marinoni, A., Horn, H. G., Keck, L., Jiang, J., Scheckman, J., McMurry, P. H., Deng, Z., Zhao, C. S., Moerman, M., Henzing, B., de Leeuw, G., Löschan, G., and Bastian, S.: Mobility particle size spectrometers: harmonization of technical standards and data structure to facilitate high quality long-term observations of atmospheric particle number size distributions, *Atmos. Meas. Tech.*, 5, 657–685, doi:10.5194/amt-5-657-2012, 2012.
- Xu, W. Y., Zhao, C. S., Ran, L., Deng, Z. Z., Liu, P. F., Ma, N., Lin, W. L., Xu, X. B., Yan, P., He, X., Yu, J., Liang, W. D., and Chen, L. L.: Characteristics of pollutants and their correlation to meteorological conditions at a suburban site in the North China Plain, *Atmos. Chem. Phys.*, 11, 4353–4369, doi:10.5194/acp-11-4353-2011, 2011.
- Young, K. C. and Warren, A. J.: A reexamination of the derivation of the equilibrium supersaturation curve for soluble particles, *J. Atmos. Sci.*, 49, 1138–1143, 1992.
- Zhao, C., Tie, X., Brasseur, G., Noone, K. J., Nakajima, T., Zhang, Q., Zhang, R., Huang, M., Duan, Y., Li, G., and Ishizaka, Y.: Aircraft measurements of cloud droplet spectral dispersion and implications for indirect aerosol radiative forcing, *Geophys. Res. Lett.*, 33, L16809, doi:10.1029/2006gl026653, 2006a.
- Zhao, C., Tie, X., and Lin, Y.: A possible positive feedback of reduction of precipitation and increase in aerosols over eastern central China, *Geophys. Res. Lett.*, 33, L11814, doi:10.1029/2006gl025959, 2006b.